

FORMAL VERIFICATION OF NOISY QUANTUM REINFORCEMENT LEARNING POLICIES

DENNIS GROSS

ABSTRACT. *Quantum reinforcement learning (QRL)* aims to leverage quantum phenomena to develop sequential decision-making policies that achieve task objectives more effectively than their classical counterparts. Unlike reinforcement learning policies implemented on classical hardware, QRL policies are subject to additional uncertainty from quantum measurements and hardware imperfections. These uncertainties, including bit-flip, phase-flip, and depolarizing noise, can alter agent behavior and lead to unsafe policy behaviour. However, there do not exist approaches that provide systematic methods for verifying *exactly* whether trained QRL policies satisfy safety requirements under specific quantum noise conditions. We present *QVerifier*, a formal verification method that uses *probabilistic model checking* to rigorously analyze trained QRL policies, with and without modeled quantum noise, to verify satisfaction or violation with safety properties. Our method incrementally constructs a formal model of the policy–environment interaction by expanding all states reachable under the policy and assigning their transition probabilities using the model’s dynamics. Quantum measurement uncertainty and optional quantum hardware noise are incorporated directly into these probabilities. The resulting model is then verified using the *Storm* model checker to assess satisfaction of the safety properties. Experiments across multiple QRL environments show that our approach precisely quantifies how different models of quantum noise affect safety guarantees. The results reveal not only how specific noise models degrade policy performance, but also cases where certain noise can improve it. By enabling rigorous safety verification before deployment, *QVerifier* addresses a critical need: because access to quantum hardware is prohibitively expensive, pre-deployment verification is essential for any safety-critical use of quantum reinforcement learning. It targets a potential classical–quantum sweet spot: trained QRL policies that execute efficiently on quantum hardware, yet remain tractable for classical probabilistic model checking despite being too slow for real-time classical deployment.

1. INTRODUCTION

As *quantum computing* [56] transitions from theory to commercial reality [46, 55, 2], it opens new opportunities for advancing *machine learning* [13, 10, 3]. *Quantum reinforcement learning (QRL)* combines *reinforcement learning (RL)* with quantum computing to train sequential decision-making policies that may achieve task objectives more effectively than their classical counterparts by leveraging quantum phenomena such as superposition and entanglement [36, 14, 50, 65, 15].

In general, an RL agent aims to learn a near-optimal policy to achieve a fixed objective by taking actions and receiving feedback in the form of rewards and state observations from the environment [67]. A policy is *memoryless* if it depends only on the current state, and it can be *stochastic*, assigning action probabilities from which the agent samples its next action.

In QRL, policies are encoded by *variational quantum circuits (VQCs)* [65], which are parameterized circuits optimized during training. A VQC takes a quantum encoding of the environment state and produces a quantum state, from which action probabilities are estimated

via repeated measurements (shots). Each shot measures the circuit on the *same encoded input*, yielding a single classical outcome by projecting the quantum state onto one of its possible results; many such shots are needed to approximate the underlying action distribution. VQCs can be executed on quantum simulators or quantum hardware [75], though simulators become exponentially slower for large circuits [16].

As research in QRL progresses into *safety-critical systems* [40, 57, 45], it is crucial to ensure that these QRL policies are developed with safety in mind [10, 66].

However, trained policies may exhibit *unsafe behavior* [22], such as collisions [9, 64], since rewards rarely capture complex safety requirements [69]. In QRL, additional uncertainty from stochastic measurements and device noise [68, 5] on costly quantum computing hardware [52] can further distort action selection.

To resolve the safety issues mentioned above, formal verification methods like *probabilistic model checking* [22] have been proposed to reason about the safety of RL on classical hardware [73, 33, 12, 30] and the correctness of quantum systems [21, 8]. Model checking is not limited by properties that rewards can express but supports a broader range of properties that can be expressed by *probabilistic computation tree logic (PCTL)* [31], a temporal logic designed to express probabilistic branching-time properties. At its core, probabilistic model checking uses mathematical models to verify a system’s correctness with respect to a given safety property [7].

However, in the context of QRL policy verification, probabilistic model checking has not yet been applied, and there are limited tools for systematic comparisons of QRL policies [38, 11, 41].

In this paper, we introduce a method, *QVerifier*, for model-checking trained QRL policies against safety properties while explicitly accounting for quantum uncertainty arising from measurements and quantum hardware noise. Given a trained QRL policy, a quantum noise model, and a formal environment model, we incrementally build a formal representation of the combined policy–noise–environment system, exploring only the states actually reachable under the trained QRL policy. We then use the probabilistic model checker *Storm* [34] to verify whether the resulting formal model satisfies the desired safety property.

Our experiments demonstrate that probabilistic model checking enables rigorous verification of trained QRL policies with and without noise with respect to safety properties, before deploying them on costly quantum hardware. We verify six policies (three QRL and three classical RL baselines) across three environments (Frozen Lake, Ski, and Freeway) under four quantum noise models: bit-flip, phase-flip, depolarizing, and amplitude damping that are applied independently at each quantum circuit gate, though *QVerifier* is not limited to these noise models. Our results reveal that noise effects are policy- and task-dependent: while bit-flip and depolarizing noise consistently degrade performance, we observe that low-level amplitude-damping noise can sometimes improve QRL policy performance, with the Ski environment showing a 27% improvement over the classical RL baseline. These findings demonstrate that pre-deployment verification not only identifies safety violations but also uncovers beneficial quantum noise regimes.

Our **main contributions** are a method for formally verifying trained QRL policy behaviors in modeled environments, with and without quantum noise models, and an exact comparison approach for QRL and classical RL performance. By enabling rigorous safety verification before deployment, *QVerifier* addresses a critical need: access to quantum hardware is prohibitively expensive, making pre-deployment verification essential for safety-critical applications. *QVerifier* targets a potential sweet spot between classical and quantum computation, where trained

QRL policies execute efficiently on quantum hardware but remain feasible to simulate classically for offline model checking. Moreover, the methodology underlying *QVerifier* could inform the design of future quantum model checkers.

2. RELATED WORK

Research at the intersection of quantum computing, machine learning, and software engineering has grown rapidly in recent years [10]. A key challenge across these areas is dealing with quantum noise, which affects both quantum circuits and the software built on top of them. Noise-aware quantum software engineering, therefore, forms an active research direction [1].

Verification of Quantum Systems. Probabilistic model checking has long been used to verify the correctness of quantum systems, such as quantum communication protocols [21] or quantum key distribution [8]. More recently, verification methods for quantum machine-learning classifier models have emerged. For example, Guan et al. propose a robustness verification method for quantum classifiers [28], and *VeriQR* provides automated robustness checking for such classifiers [44]. However, none of these works apply probabilistic model checking to the verification of *QRL policies*.

Verification of Classical RL Policies. In RL on classical hardware, several works study the verification of trained RL policies [19, 39, 17, 18, 76, 37]. A particularly relevant line of work, for this paper, uses probabilistic model checking to verify deep RL policies [22, 25, 42]. *COOL-MC* [22] introduced incremental model construction for RL policies and safety verification with the *Storm* model checker. Our work builds directly on this idea but extends it to handle QRL policies, including quantum measurements and hardware noise.

Noise and Robustness in RL and QRL. Classical noise has also been studied in the context of classical RL, where perturbations typically affect the agent’s state observations rather than the policy’s inner workings [24, 23]. In contrast, QRL naturally introduces additional uncertainty from quantum-state measurements and noise arising from error-prone quantum circuit gates within the quantum circuit.

For improving robustness of QRL during training, *RegQPG* adds Lipschitz regularization to the policy gradient objective [49]. Unlike this training-time approach, we perform *post-training verification* to check whether a trained QRL policy satisfies a safety property under explicit hardware noise models (bit-flip, phase-flip, depolarizing, amplitude-damping).

Several works analyze how quantum noise affects QRL performance. Skolik et al. study realistic noise sources, including shot noise, coherent Gaussian noise, and decoherence, and show that their effects vary strongly with both the type and the magnitude of the noise [66]. These insights motivate our goal of *exactly* verifying trained QRL policies *under specific noise models*, rather than studying robustness in aggregate.

Other Related Directions. Some research modifies trained RL policy architecture by disrupting parts of it during verification [26], but this differs from having QVC gate-level noise. Closely related to verification is testing, with extensive work on both testing quantum systems and using quantum computing for testing [71, 54, 70, 58, 48, 72, 4].

Summary. While verification techniques exist for quantum systems, quantum classifiers, and classical RL policies, no prior work uses probabilistic model checking to verify *memoryless QRL policies* under different quantum noise models. Our work fills this gap by introducing a QRL-specific model-checking method.

3. BACKGROUND

First, we outline how sequential decision-making tasks can be formally represented as *Markov decision processes (MDPs)*, and how memoryless stochastic policies and their properties can be verified with this method. Second, we introduce quantum circuits and describe how to model relevant sources of quantum noise. Finally, we present quantum REINFORCE, a QRL method for training sequential decision-making policies.

3.1. Probabilistic Systems. A *probability distribution* over a set X is a function $\mu: X \rightarrow [0, 1]$ with $\sum_{x \in X} \mu(x) = 1$. The set of all distributions on X is $\text{Distr}(X)$.

Definition 1 (MDP). A MDP is a tuple $M = (S, s_0, \text{Act}, \text{Tr}, \text{rew}, \text{AP}, L)$ where S is a finite, nonempty set of states; $s_0 \in S$ is an initial state; Act is a finite set of actions; $\text{Tr}: S \times \text{Act} \rightarrow \text{Distr}(S)$ is a partial probability transition function and $\text{Tr}(s, a, s')$ denotes the probability of transitioning from state s to state s' when action a is taken; $\text{rew}: S \times \text{Act} \rightarrow \mathbb{R}$ is a reward function; AP is a set of atomic propositions; $L: S \rightarrow 2^{\text{AP}}$ is a labeling function.

We represent each state $s \in S$ as a vector of d integer features (f_1, \dots, f_d) , where $f_i \in \mathbb{Z}$. The available actions in $s \in S$ are $\text{Act}(s) = \{a \in \text{Act} \mid \text{Tr}(s, a) \neq \perp\}$ where $\text{Tr}(s, a) \neq \perp$ is defined as action a at state s does not have a transition (action a is not available in state s). In our setting, we assume that all actions are available at all states.

Definition 2 (Memoryless Stochastic Policy). A memoryless stochastic policy π for an MDP M is a function

$$\pi: S \rightarrow \text{Distr}(\text{Act}),$$

i.e., for each state $s \in S$, $\pi(s)$ is a probability distribution over actions. Equivalently, this can be expressed as

$$\pi(a \mid s) = \pi(s)(a) \in [0, 1], \quad \sum_{a \in \text{Act}} \pi(a \mid s) = 1,$$

where $\pi(a \mid s)$ denotes the probability of selecting action a when in state s .

Applying a memoryless stochastic policy π to an MDP M yields an *induced discrete-time Markov chain (DTMC)* whose transition probabilities combine the MDP's probabilistic dynamics and the policy's stochastic choice of actions.

Definition 3 (Induced DTMC). Given an MDP $M = (S, s_0, \text{Act}, \text{Tr}, \text{rew}, \text{AP}, L)$ and a stochastic policy π , the induced DTMC is $M^\pi = (S, s_0, P^\pi, \text{AP}, L)$ where the transition probability function $P^\pi: S \times S \rightarrow [0, 1]$ is defined by marginalizing over actions

$$P^\pi(s, s') = \sum_{a \in \text{Act}(s)} \pi(a \mid s) \cdot \text{Tr}(s, a, s').$$

The transition probability $P^\pi(s, s')$ represents the total probability of moving from state s to state s' by summing over all actions weighted by their selection probabilities under policy π .

3.2. Probabilistic Model Checking. Storm [34] is a model checker. It enables the verification of properties in induced DTMCs, with reachability properties being among the most fundamental. These properties assess the probability of a system reaching a particular state. For example, one might ask, “Is the probability of the system reaching an unsafe state less than 0.1?” A property can be either *satisfied* or *violated*.

The *general workflow* for model checking with Storm is as follows (see also Figure 1): First, the system, in our setting, an induced DTMC, is modeled using a language such as PRISM [60]. Next, a property is formalized based on the system’s requirements. Using these inputs, the model checker Storm verifies whether the formalized property holds or fails within the model.

In probabilistic model checking, there is no universal “one-size-fits-all” solution [34]. The most suitable tools and techniques depend on the specific input model and properties being analyzed. During model checking, Storm can proceed “on the fly”, exploring only the parts of the DTMC most relevant to the formal verification.

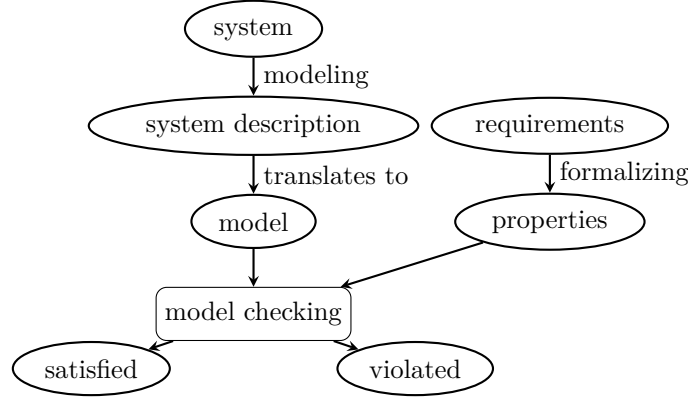


FIGURE 1. General model checking workflow [34]. First, the system needs to be formally modeled, for instance, via PRISM. Then, the requirements are formalized, for instance, via PCTL. Eventually, both are inputted into the model checker, like Storm, which verifies the property.

Properties verifiable via Storm include temporal logic formulas for DTMCs, defined on paths using PCTL [32], a branching-time logic.

Although it is not formally allowed in PCTL, Storm can still be used to request the probability of fulfilling a path formula from each state. Rather than simply checking whether certain PCTL properties, such as $P_{=1}(F \text{ collision})$, are satisfied, which would indicate that the system reaches the *collision* state with probability 1, we can query Storm to compute the actual probability value, denoted as $P(F \text{ collision})$, which in this case equals 1.

In this paper, we consider the *eventually* path property F , which states that a property holds at some future state along a path. Its syntax is

$$P_{\sim p}(F \varphi)$$

meaning that the probability of reaching a state where φ holds, along a path starting from the initial state, satisfies the bound $\sim p$, where \sim is a comparison operator such as $<$, \leq , \geq , or $>$, and p is a probability threshold.

We also consider the *until* path property U , which is more expressive than simple reachability. The until property states that a condition φ holds along a path until a state satisfying ψ is reached. Its syntax is

$$P_{\sim p}(\varphi U \psi)$$

meaning that the probability of reaching a state where ψ holds, while φ holds continuously along the path until that point, satisfies the bound $\sim p$.

3.3. Quantum Computing. A quantum state $|\psi\rangle$ of a system is represented by a unit vector in a complex Hilbert space \mathcal{H} . This is $\mathcal{H} = \mathbb{C}^2$ for a single qubit system [56]. In Dirac notation, $|\psi\rangle$ is called a *ket* and represents a column vector, while its dual $\langle\psi|$ is called a *bra* and represents the corresponding conjugate transpose (row vector). The inner product between two states is written as $\langle\phi|\psi\rangle$, and the outer product $|\phi\rangle\langle\psi|$ forms a matrix.

More generally, quantum systems can be represented by a *density matrix* $\rho = |\psi\rangle\langle\psi|$. Density matrices are essential for describing mixed states (statistical mixtures of pure states) and systems affected by noise, which cannot be represented by a single state vector. For a general mixed state, we have

$$\rho = \sum_i p_i |\psi_i\rangle\langle\psi_i|,$$

where $\{p_i\}$ are classical probabilities ($p_i \geq 0$, $\sum_i p_i = 1$).

Every valid density matrix satisfies three key properties: it is *Hermitian*, meaning it is equal to its conjugate transpose and thus has real eigenvalues; *positive semidefinite*, ensuring that all probabilities are non-negative; and has *unit trace*, ensuring that probabilities of all measurement outcomes sum to one.

3.3.1. Entanglement. A multi-qubit quantum state is called *entangled* if it cannot be written as a tensor product of individual qubit states. For a two-qubit system, a state $|\psi\rangle \in \mathcal{H}_A \otimes \mathcal{H}_B$ is *separable* if it can be expressed as

$$|\psi\rangle = |\phi\rangle_A \otimes |\chi\rangle_B,$$

and *entangled* otherwise. Entangled states produce measurement correlations that are impossible to replicate with any classical system [62].

3.3.2. Amplitude encoding. A common technique for encoding classical data vectors into quantum states is *amplitude encoding* [38]. Given a classical state $s \in S$ with d components, amplitude encoding prepares a quantum state

$$|\psi\rangle = \sum_{i=0}^{d-1} \tilde{s}_i |e_i\rangle,$$

where $\{|e_i\rangle\}_{i=0}^{d-1}$ is an orthonormal basis for $\mathcal{H} = \mathbb{C}^d$, and $\tilde{s}_i = s_i/\|s\|$ are the normalized amplitudes, ensuring $\sum_i |\tilde{s}_i|^2 = 1$.

3.3.3. Quantum channels. Quantum evolution is described by a *quantum channel*, a linear, completely positive, and trace-preserving map $\mathcal{E} : \rho \mapsto \rho'$. Every quantum channel admits a *Kraus representation*

$$\mathcal{E}(\rho) = \sum_i K_i \rho K_i^\dagger,$$

where $\{K_i\}$ are Kraus operators satisfying $\sum_i K_i^\dagger K_i = I$. The *completely positive* property ensures that the map remains physical when applied to subsystems, while *trace-preserving* guarantees that probabilities sum to one.

Unitary evolution. The special case of *noiseless* quantum evolution corresponds to a single Kraus operator $K = U$, where U is a *unitary operator* satisfying $U^\dagger U = U U^\dagger = I$. The

channel becomes

$$\mathcal{E}(\rho) = U\rho U^\dagger.$$

Unitary operations are *reversible* (applying U^\dagger inverts the operation) and preserve quantum coherence.

Pauli operators. The Pauli operators $\{X, Y, Z\}$ are fundamental single-qubit operators:

$$X = \begin{pmatrix} 0 & 1 \\ 1 & 0 \end{pmatrix}, \quad Y = \begin{pmatrix} 0 & -i \\ i & 0 \end{pmatrix}, \quad Z = \begin{pmatrix} 1 & 0 \\ 0 & -1 \end{pmatrix}.$$

These operators are both Hermitian ($P^\dagger = P$) and unitary ($P^\dagger P = I$).

3.3.4. Noisy channels. These channels arise when quantum systems interact with their environment and require multiple Kraus operators. Each K_i corresponds to a possible outcome of an interaction with the environment or an error process. Noisy channels with multiple Kraus operators are *irreversible*. Different physical noise processes correspond to specific choices of Kraus operators.

- *Bit-flip noise:*

$$\mathcal{E}_{\text{BF}}(\rho) = (1 - p)\rho + p X\rho X,$$

where p is the bit-flip probability.

- *Phase-flip noise:*

$$\mathcal{E}_{\text{PF}}(\rho) = (1 - p)\rho + p Z\rho Z.$$

- *Depolarizing noise:*

$$\mathcal{E}_{\text{DP}}(\rho) = (1 - p)\rho + \frac{p}{3}(X\rho X + Y\rho Y + Z\rho Z).$$

- *Amplitude damping noise:*

$$\mathcal{E}_{\text{AD}}(\rho) = E_0\rho E_0^\dagger + E_1\rho E_1^\dagger,$$

with Kraus operators

$$E_0 = \begin{pmatrix} 1 & 0 \\ 0 & \sqrt{1 - \gamma} \end{pmatrix}, \quad E_1 = \begin{pmatrix} 0 & \sqrt{\gamma} \\ 0 & 0 \end{pmatrix},$$

where γ denotes the damping rate, representing the probability of energy loss from the excited to the ground state.

3.3.5. Computing measurement probabilities analytically. When modeling a quantum circuit analytically (e.g., using exact matrix calculations and noise models), the measurement probabilities can be directly extracted from the final density matrix ρ_{final} .

For computational basis measurements, the probability of measuring outcome x is simply given by the corresponding diagonal element

$$p_x = \langle x | \rho_{\text{final}} | x \rangle = (\rho_{\text{final}})_{xx}.$$

For a single qubit, this means

$$p_0 = \rho_{00}, \quad p_1 = \rho_{11}.$$

For an n -qubit system, the density matrix is $2^n \times 2^n$, and the probability of measuring bitstring $x \in \{0, 1\}^n$ is the diagonal element at the corresponding index.

3.3.6. *Multi-shot experiments.* On quantum hardware, the outcome of a quantum measurement is inherently probabilistic: each circuit execution (or *shot*) yields a single bitstring sampled from the probability distribution p_x . To estimate these probabilities, one repeats the circuit many times (a process known as performing a *multi-shot experiment*). After N shots, the empirical frequencies $\hat{p}_x = n_x/N$ (where n_x is the count of outcome x) approximate the true probabilities p_x .

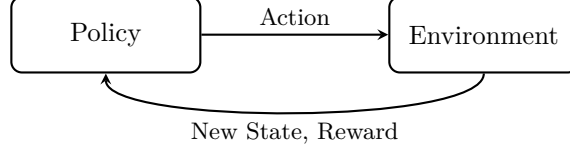


FIGURE 2. An RL agent interacts with an environment. The agent sends an action and receives the resulting state and reward, closing the feedback loop. The interaction ends when a terminal state is reached.

3.4. **Quantum REINFORCE.** REINFORCE [74] is a policy gradient RL algorithm that trains a parameterized policy π_θ by directly optimizing the expected cumulative reward (see Figure 2). Given the reward function rew from Definition 1, the *return* G_t from time step t is the discounted sum of rewards along a trajectory

$$G_t = \sum_{k=t}^T \gamma^{k-t} rew(s_k, a_k),$$

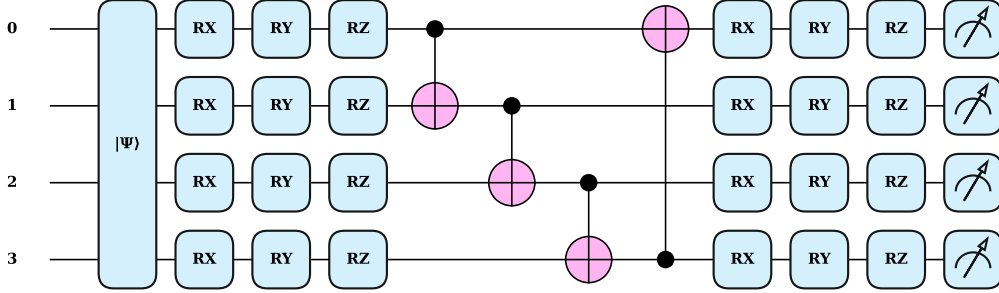


FIGURE 3. An example of a variational quantum circuit architecture for a quantum REINFORCE agent. The circuit operates on four qubits and has two variational layers with 24 trainable parameters (gates with name R*). State preparation encodes the input via amplitude encoding to the qubits. Layer 0 contains rotation gates (RX, RY, RZ) and CNOT entanglement in ring topology. Layer 1 contains only rotations. Pauli-Z measurements produce expectation values that are classically post-processed into action probabilities via a softmax function.

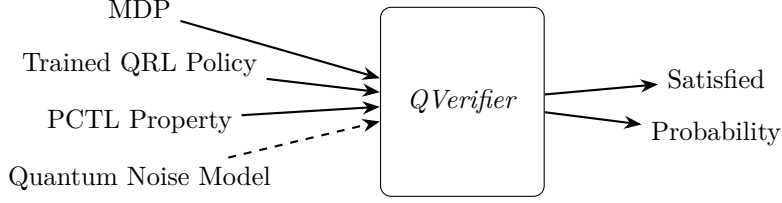


FIGURE 4. Given an MDP, a trained QRL policy, a PCTL property, and, optionally, quantum noise models as inputs, the method outputs whether the safety property is satisfied and its exact probability.

where T is the episode length and $\gamma \in [0, 1]$ is the discount factor. The policy gradient theorem gives

$$\nabla_{\theta} J(\theta) = \mathbb{E}_{\pi_{\theta}} \left[\sum_{t=0}^T \nabla_{\theta} \log \pi_{\theta}(a_t | s_t) \cdot G_t \right],$$

where $J(\theta)$ is the expected return and the expectation is over trajectories sampled from policy π_{θ} . Parameters are updated via gradient ascent using sampled trajectories.

In *Quantum REINFORCE*, the policy π_{θ} is implemented as a parameterized quantum circuit (see Figure 3), where θ represents quantum gate parameters [63]. For state s , the circuit prepares a density matrix $\rho_{\theta}(s)$. Performing a computational basis measurement yields action probabilities

$$\pi_{\theta}(a | s) = \langle a | \rho_{\theta}(s) | a \rangle = \text{Tr}(|a\rangle \langle a| \rho_{\theta}(s)).$$

The gradient $\nabla_{\theta} \log \pi_{\theta}(a | s)$ is computed using parameter-shift rules [51], and parameters are updated following standard REINFORCE.

Given a policy π with parameters θ and a noise channel \mathcal{E} , action selection for state s proceeds as follows. The state s is encoded into an initial density matrix $\rho_0(s)$, which is then transformed by the trained unitary circuit U_{θ} to produce $\rho = U_{\theta} \rho_0(s) U_{\theta}^{\dagger}$. The noise channel is applied to yield the noisy density matrix $\rho' = \mathcal{E}(\rho)$, and measurement gives action probabilities

$$\pi_{\theta}^{\mathcal{E}}(a | s) = \langle a | \mathcal{E}(U_{\theta} \rho_0(s) U_{\theta}^{\dagger}) | a \rangle.$$

4. METHODOLOGY

As illustrated in Figure 4, our method, *QVerifier*, takes as input: (i) an MDP representing the environment dynamics, (ii) a trained QRL policy, (iii) a PCTL property specifying the desired safety requirement, and (iv) an optional quantum noise model capturing hardware imperfections. *QVerifier* verifies whether the policy satisfies or violates the property and quantifies the probability for it. Our approach consists of two internal stages (see also Algorithm 1): (i) constructing the induced DTMC, and (ii) performing probabilistic model checking of the built formal model.

4.1. Induced DTMC Construction. Given an MDP $M = (S, s_0, Act, Tr, rew, AP, L)$ and a memoryless stochastic policy π , where $\pi(a | s)$ denotes the probability of selecting action a in state s , we construct an induced DTMC M^{π} that resolves all nondeterminism. The transition

Algorithm 1 QVerifier: Formal Verification of QRL Policies

Require: MDP $M = (S, s_0, Act, Tr, rew, AP, L)$

Require: Trained QRL policy π_θ

Require: PCTL property φ

Ensure: Satisfaction result and probability p

Stage 1: Induced DTMC Construction

1: $M^\pi \leftarrow \text{BUILDDTMC}(s_0, \emptyset)$

Stage 2: Probabilistic Model Checking

2: $(result, p) \leftarrow \text{STORM.verify}(M^\pi, \varphi)$

3: **return** $(result, p)$

4: **procedure** $\text{BUILDDTMC}(s, Visited)$

5: **if** $s \in Visited$ **or** s is not relevant for φ **then**

6: **return**

7: **end if**

8: $Visited \leftarrow Visited \cup \{s\}$

9: **for all** $s' \in S$ where $P^\pi(s, s') > 0$ **do**

10: Compute $P^\pi(s, s') = \sum_{a \in Act(s)} \pi_\theta(a \mid s) \cdot Tr(s, a, s')$

11: $\text{BUILDDTMC}(s', Visited)$

12: **end for**

13: **end procedure**

probability between any two states $s, s' \in S$ is computed by marginalizing over all actions:

$$(1) \quad P^\pi(s, s') = \sum_{a \in Act(s)} \pi(a \mid s) \cdot Tr(s, a, s').$$

We build M^π incrementally starting from the initial state s_0 . For each reachable state s , we consider all actions a with non-zero policy probability ($\pi(a \mid s) > 0$). For each such action, we expand all successor states s' where $Tr(s, a, s') > 0$ and compute their transition probabilities using Equation (1). This process continues until no new states are discovered. It terminates early once all states relevant to the PCTL property verification have been visited, avoiding unnecessary state expansion that does not affect the verification result.

To assess the impact of a specific quantum noise model, we follow the same procedure in Algorithm 1 using the noisy policy $\pi_\theta^\mathcal{E}$ instead of the policy π_θ . This constructs a separate induced DTMC that captures how hardware imperfections affect the policy's behavior. Figure 6 illustrates this process for a specific state: starting from state s_0 , the blue solid arrows show transitions from the noise-free policy, while the red dashed arrows show how the modeled quantum noise alters the transition probabilities in the action sampling process.

4.2. Verification. The resulting induced DTMC fully encodes the QRL policy's probabilistic behavior (with and without a quantum noise model), enabling formal verification using the Storm model checker. Storm verifies whether the specified PCTL property holds and computes exact satisfaction probabilities.

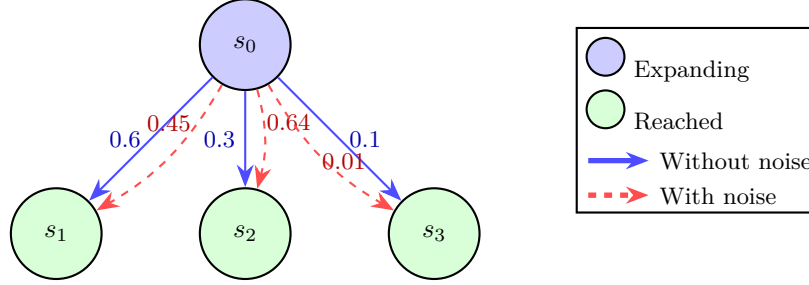


FIGURE 5. One expansion step in the incremental DTMC construction, showing two example DTMCs overlaid for comparison. Starting from state s_0 , the policy samples an action which leads to successor states s_1 , s_2 , and s_3 . Blue solid arrows represent the DTMC constructed from the noise-free policy, while red dashed arrows represent a separate DTMC constructed from the noisy policy $\pi_\theta^\mathcal{E}$, illustrating how the quantum noise model in the action sampling process alters the transition probabilities. This expansion process is repeated for each new state until all states reachable by the policy have been visited.

4.3. Limitations. Our approach supports verifying any memoryless stochastic quantum policy, but it has several constraints. We are restricted to discrete state and action spaces [22]. The size of the parameterized quantum circuit also poses scalability limits [16]. Additionally, time-dependent noise effects such as thermal relaxation [35] cannot be modeled due to the Markovian property of our formalism [22].

5. EXPERIMENTS

In this section, we empirically evaluate the verification of QRL policies using probabilistic model checking. Our experiments are designed to address the following research questions:

- **RQ1:** How do quantum and classical policy verification compare?
- **RQ2:** How does quantum noise affect QRL policies?

To answer these research questions, we evaluate trained classical and quantum policies across three benchmark environments and verify them against safety properties expressed in PCTL.

We structure our analysis as follows. First, we compare classical REINFORCE with noise-free quantum REINFORCE verification to assess performance differences and potential safety violations. Second, we incorporate realistic quantum noise models directly into the verification process to study how gate-level noise propagates through the induced stochastic policy and affects key safety-relevant properties.

5.1. Setup. We now describe our setup. First, we describe the used environments, then the trained policies, and finally, our technical setup.

5.1.1. Environments. The *Frozen Lake* environment is a commonly used OpenAI gym benchmark, where the agent has to reach the goal (frisbee) on a frozen lake (reward +1). The agent’s movement direction is partially uncertain.

The *Ski* environment uses a 4-bit state representation encoding the integers 0 to 15, with the agent starting in state 1 and choosing between two actions called left and right. Transitions depend on whether the current state is odd or even: odd states advance through left and even

TABLE 1. Comparison between QRL and classical RL in probabilistic model checking. The table reports, for each environment and PCTL property, the verification result, the number of explored states and transitions, and the total verification time (building time + model checking time).

Setup		QRL Policy Model Checking				RL Policy Model Checking			
Env.	PCTL Query	Result	States	Transitions	Time (s)	Result	States	Transitions	Time (s)
Freeway	P(F Goal)	0.621	496	2080	84	0.7	496	2080	4
Frozen Lake	P(F Goal)	0.03	17	48	6	0.04	17	48	0.2
Frozen Lake	$P(pos \leq 3 \cup pos = 7)$	0.124	8	18	1.19	0.061	8	18	0.05
Ski	P(F Goal)	0.437	7	12	0.5	0.45	7	12	0.03

states advance through right, while incorrect choices often send the agent back to state 0, which represents a crash. State 6 serves as the goal and absorbs both actions. Rewards are given when the agent selects the action that correctly advances the current state rather than returning to zero, creating a simple parity-based navigation task toward the goal.

In the *Freeway* environment, the RL agent controls a chicken (up, down, or no operation) running across a highway filled with traffic to get to the other side. Every time the chicken gets across the highway, it earns a reward of one. An episode ends if the chicken gets hit by a car or reaches the other side. Each state is an image of the game’s state. Note that we use an abstraction of the original game, which sets the chicken into the middle column of the screen and contains fewer pixels than the original game, but uses the same reward function and actions [25].

5.1.2. Trained policies. In each environment, we train a classical REINFORCE agent and a quantum-enhanced REINFORCE agent with similar training conditions. Both agents are trained for the same number of epochs (always 10,000 epochs), and we use identical reward structures. While our focus is on these two types of REINFORCE agents, the approach generalizes to other memoryless QRL policies [50]. Note that we did not focus on archiving high-performing agents, as this paper focuses on the verification process itself. For details about the exact training source code, we refer to the technical setup.

5.1.3. Technical setup. We executed our benchmarks in a Docker container with 16 GB RAM, and an AMD Ryzen 7 7735hs with Radeon graphics \times 16 processor with the operating system Ubuntu 20.04.5 LTS. For model checking, we use Storm 1.7.1 (dev). For the quantum circuit, we use PennyLane 0.42.3. Implementation details are provided in the accompanying source code <https://github.com/LAVA-LAB/COOL-MC/tree/qverifier>.

5.2. Analysis. First, we do a comparative performance analysis between classical REINFORCE and quantum REINFORCE verification. Second, we analyze how different quantum noise models influence the trained quantum REINFORCE policies.

RQ1: How do quantum and classical policy verification compare? Table 1 summarizes the verification outcomes for both classical and quantum policies. For each environment, we report the reachability probability (i.e., the likelihood that the policy reaches the target state) and a more complex until property (i.e., the likelihood that the policy reaches a specific state while satisfying a given condition along the path), the number of states and transitions explored during model checking, and the total verification time.

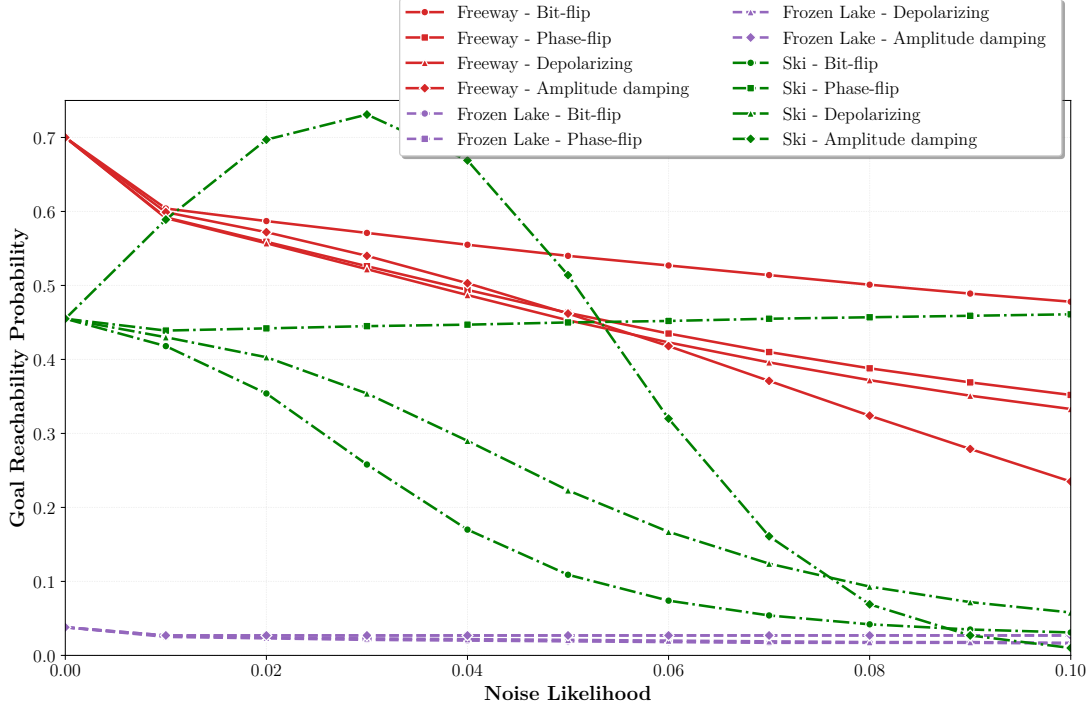


FIGURE 6. *Performance changes of the quantum policies under increasing noise likelihoods for the goal-reachability probabilities. The x -axis denotes the noise likelihoods, while the y -axis indicates the corresponding performance metric (higher is better).*

Across all environments, classical REINFORCE policies outperform their quantum counterparts in terms of reachability probability. This performance gap may be attributed to the limited expressivity of shallow variational circuits or to optimization challenges inherent in quantum policy gradient methods. Considering the complex safety requirement, expressed via the until-formula $P(pos \leq 3 \cup pos = 7)$, which represents the unsafe behavior of the agent traversing the top border leftward before falling into the water hole at position 7, we find that the QRL policy violates this safety requirement more often than the RL policy.

Quantum policies consistently exhibit longer verification times than classical policies, primarily due to the computational overhead of the quantum circuit at each verification state.

The induced DTMC sizes (states and transitions) are identical for QRL and classical RL policies in each environment, since both assign non-zero probability to all actions, making the same states reachable; only the transition probabilities differ. However, DTMC sizes can differ when certain actions have zero probability.

These results suggest that, under ideal (noise-free) conditions, classical policies remain more effective for the tasks considered. However, as discussed in the following section, introducing realistic noise models can alter this comparison, sometimes leading to scenarios in which quantum policies outperform classical policies.

RQ2: How does quantum noise affect QRL policies? To evaluate how quantum hardware imperfections affect policy reliability, we conduct experiments using a gate-level noise model integrated directly into the policy verification procedures, focusing on the goal-reachability probabilities across the different environments.

In our experiment, at *every* encountered state s , the agent computes its action distribution by executing the full noisy quantum circuit. Concretely, the process consists of: (i) encoding the classical state s into the quantum amplitudes, (ii) executing the variational quantum circuit with noise inserted after each gate, and (iii) obtaining the stochastic policy $\pi_\theta^\mathcal{E}$. In this setup, noise accumulates proportionally to the circuit depth, so deeper circuits experience greater degradation.

Figure 6 shows how performance changes across environments as the probability of applying noise at each gate increases. We study several standard noise channels: bit-flip, phase-flip, depolarizing, and amplitude damping. The verification results vary across noise types.

Bit-flip noise inverts computational basis states, causing performance loss across all tasks.

Depolarizing noise introduces a uniform mixture of Pauli errors, pushing quantum states toward maximal randomness and resulting in the strongest overall degradation.

Phase-flip noise, which affects only relative phases while leaving populations unchanged, shows a slight performance improvement for the QRL Ski policy.

Finally, we observe an effect under low levels of amplitude-damping noise: in the Ski environment, performance increases and even surpasses the trained classical RL baseline by 27% (see Table 1 for comparison). This beneficial regime disappears as noise levels increase, suggesting that mild dissipation can occasionally stabilize or regularize quantum policies, whereas stronger noise ultimately degrades performance. These observations align with prior findings [36], which similarly report noise-induced performance enhancements.

6. DISCUSSION

QVerifier addresses the high cost and limited availability of quantum hardware [47, 52]: verifying QRL policies classically avoids the expense of on-device testing [52]. QRL policy verification reveals potential safety violations, shows how a specific quantum noise model affects policy behavior, and supports deployment decisions.

A key feature is the *exact* analytical treatment of quantum noise. Instead of relying on empirical sampling, we compute action probabilities directly from the density matrix, yielding noise-dependent exact transition probabilities. This enables continuous noise-parameter sweeps and precise analysis of how safety properties change with different noise likelihoods (see Figure 6).

The resulting noise-safety profiles guide hardware selection [59]. If, for example, a policy remains safe up to a depolarizing rate of $p = 0.05$, practitioners can choose devices whose gate fidelities meet this requirement and allocate error budgets accordingly.

A fundamental tension underlies any classical verification of quantum systems [6, 50, 11]: if a circuit is small enough to compute efficiently, one might question the benefit of quantum execution; if it is too large, classical verification becomes too costly [16].

Nevertheless, *QVerifier* targets a *sweet spot*: trained QRL policies that run efficiently on quantum hardware but would be far too slow for real-time execution on classical devices, while still remaining computable on classical hardware for model checking, where extended computation time is acceptable. However, this sweet spot remains to be demonstrated in practice; characterizing its boundaries and showing that relevant problems fall within it is essential for validating *QVerifier*’s real-world applicability.

When full environment verification is infeasible, *QVerifier* still supports targeted debugging. Practitioners can analyze critical regions of the state space to locate unsafe behaviors.

Another advantage of *QVerifier* is that it can also be used to analyze different QRL policy designs [50], enabling systematic comparisons [11] of how architectural choice, such as circuit depth [20], encoding schemes [61], or measurement strategies [43], impact robustness under noise [49] and adherence to safety requirements, including for smaller quantum circuits. Note that *QVerifier* can also be used without quantum noise, which is particularly relevant for quantum-inspired reinforcement learning [29] approaches that employ quantum formalizations in their classical policy design without requiring quantum hardware.

Beyond its immediate applications, *QVerifier* may inform the design of future quantum model checkers [8].

7. CONCLUSION

We proposed *QVerifier*, a method for formally verifying trained QRL policies against safety properties while accounting for quantum measurement uncertainty and quantum noise. We validated our method across multiple scenarios with and without quantum noise models.

Future work includes integrating explainable RL methods to attribute safety performance to specific gates and circuit elements [26], using model-checking feedback to guide training so that QRL agents learn better policies [27], and quantum noise mitigation [53] for QRL.

ACKNOWLEDGEMENTS

I thank *Shaukat Ali* for his valuable feedback, his expertise, and his time. His guidance helped shape several key ideas and greatly improved the clarity and quality of the final presentation.

REFERENCES

- [1] Shaukat Ali. Dependable and noise-aware quantum software engineering, 2022.
- [2] Shaukat Ali and Énaüt Mendiluze. Towards real-world quantum computing applications, 2025.
- [3] Shaukat Ali, Xinyi Wang, Asmar Muqet, and Énaüt Mendiluze. Ai for quantum & quantum for ai, 2025.
- [4] Hugo Araujo, Xinyi Wang, Mohammad Mousavi, and Shaukat Ali. Using quantum annealing to generate test cases for cyber-physical systems. *arXiv preprint arXiv:2504.21684*, 2025.
- [5] Aviv Aroch, Ronnie Kosloff, and Shimshon Kallush. Mitigating controller noise in quantum gates using optimal control theory. *Quantum*, 8:1482, 2024.
- [6] Ryan Babbush, Robbie King, Sergio Boixo, William Huggins, Tanuj Khattar, Guang Hao Low, Jarrod R McClean, Thomas O’Brien, and Nicholas C Rubin. The grand challenge of quantum applications. *arXiv preprint arXiv:2511.09124*, 2025.
- [7] Christel Baier and Joost-Pieter Katoen. *Principles of model checking*. MIT press, 2008.
- [8] Pedro Baltazar, Rohit Chadha, and Paulo Mateus. Quantum computation tree logic—model checking and complete calculus. *International Journal of Quantum Information*, 6(02):219–236, 2008.
- [9] Jian Ban and Gongyan Li. Training is execution: A reinforcement learning-based collision avoidance algorithm for volatile scenarios. *IEEE Access*, 12:116956–116967, 2024.
- [10] Muneera Bano, Shaukat Ali, and Didar Zowghi. Envisioning responsible quantum software engineering and quantum artificial intelligence. *Automated Software Engineering*, 32(2):69, 2025.
- [11] Joseph Bowles, Shah Nawaz Ahmed, and Maria Schuld. Better than classical? the subtle art of benchmarking quantum machine learning models. *arXiv preprint arXiv:2403.07059*, 2024.
- [12] Tomáš Brázdil, Krishnendu Chatterjee, Martin Chmelik, Vojtěch Forejt, Jan Kretínský, Marta Z. Kwiatkowska, David Parker, and Mateusz Ujma. Verification of markov decision processes using learning algorithms. In *ATVA*, volume 8837 of *LNCS*, 2014.
- [13] Marco Cerezo, Guillaume Verdon, Hsin-Yuan Huang, Lukasz Cincio, and Patrick J. Coles. Challenges and opportunities in quantum machine learning. *Nat. Comput. Sci.*, 2(9):567–576, 2022.

- [14] Samuel Yen-Chi Chen. An introduction to quantum reinforcement learning (qrl). In *2024 15th International Conference on Information and Communication Technology Convergence (ICTC)*, pages 1139–1144. IEEE, 2024.
- [15] Kalyan Cherukuri, Aarav Lala, and Yash Yardi. Q-policy: Quantum-enhanced policy evaluation for scalable reinforcement learning. *CoRR*, abs/2505.11862, 2025.
- [16] Alessio Cicero, Mohammad Ali Maleki, Muhammad Waqar Azhar, Anton Frisk Kockum, and Pedro Trancoso. Simulation of quantum computers: Review and acceleration opportunities. *CoRR*, abs/2410.12660, 2024.
- [17] Davide Corsi, Enrico Marchesini, and Alessandro Farinelli. Formal verification of neural networks for safety-critical tasks in deep reinforcement learning. In Cassio de Campos and Marloes H. Maathuis, editors, *Proceedings of the Thirty-Seventh Conference on Uncertainty in Artificial Intelligence*, volume 161 of *Proceedings of Machine Learning Research*, pages 333–343. PMLR, 27–30 Jul 2021.
- [18] Klaus Dräger, Vojtech Forejt, Marta Z. Kwiatkowska, David Parker, and Mateusz Ujma. Permissive controller synthesis for probabilistic systems. *Log. Methods Comput. Sci.*, 11(2), 2015.
- [19] Tomer Eliyahu, Yafim Kazak, Guy Katz, and Michael Schapira. Verifying learning-augmented systems. In *SIGCOMM*, pages 305–318. ACM, 2021.
- [20] Thomas Fösel, Murphy Yuezhen Niu, Florian Marquardt, and Li Li. Quantum circuit optimization with deep reinforcement learning. *arXiv preprint arXiv:2103.07585*, 2021.
- [21] Simon Gay, Rajagopal Nagarajan, and Nikolaos Papanikolaou. Probabilistic model-checking of quantum protocols. *arXiv preprint quant-ph/0504007*, 2005.
- [22] Dennis Gross, Nils Jansen, Sebastian Junges, and Guillermo A. Pérez. COOL-MC: A comprehensive tool for reinforcement learning and model checking. In *SETTA*, volume 13649 of *Lecture Notes in Computer Science*, pages 41–49. Springer, 2022.
- [23] Dennis Gross, Christoph Schmidl, Nils Jansen, and Guillermo A. Pérez. Model checking for adversarial multi-agent reinforcement learning with reactive defense methods. In *ICAPS*, pages 162–170. AAAI Press, 2023.
- [24] Dennis Gross, Thiago D. Simão, Nils Jansen, and Guillermo A. Pérez. Targeted adversarial attacks on deep reinforcement learning policies via model checking. In *ICAART (3)*, pages 501–508. SCITEPRESS, 2023.
- [25] Dennis Gross and Helge Spieker. Probabilistic model checking of stochastic reinforcement learning policies. In *ICAART (3)*, pages 438–445. SCITEPRESS, 2024.
- [26] Dennis Gross and Helge Spieker. Safety-oriented pruning and interpretation of reinforcement learning policies. In *ESANN*, 2024.
- [27] Shangding Gu, Long Yang, Yali Du, Guang Chen, Florian Walter, Jun Wang, and Alois Knoll. A review of safe reinforcement learning: Methods, theories and applications. *IEEE Transactions on Pattern Analysis and Machine Intelligence*, 2024.
- [28] Ji Guan, Wang Fang, and Mingsheng Ying. Robustness verification of quantum classifiers. In *CAV (1)*, volume 12759 of *Lecture Notes in Computer Science*, pages 151–174. Springer, 2021.
- [29] Alireza Habibi, Saeed Ghoorchian, and Setareh Maghsudi. Quantum-inspired reinforcement learning in the presence of epistemic ambivalence. *arXiv preprint arXiv:2503.04219*, 2025.
- [30] Ernst Moritz Hahn, Mateo Perez, Sven Schewe, Fabio Somenzi, Ashutosh Trivedi, and Dominik Wojtczak. Omega-regular objectives in model-free reinforcement learning. In *TACAS (1)*, volume 11427 of *LNCS*, pages 395–412. Springer, 2019.
- [31] Hans Hansson and Bengt Jonsson. A logic for reasoning about time and reliability. *Formal aspects of computing*, 6(5):512–535, 1994.
- [32] Hans Hansson and Bengt Jonsson. A logic for reasoning about time and reliability. *Formal Aspects Comput.*, 6(5):512–535, 1994.
- [33] Mohammadhosein Hasanbeig, Daniel Kroening, and Alessandro Abate. Deep reinforcement learning with temporal logics. In *FORMATS*, volume 12288 of *LNCS*, 2020.
- [34] Christian Hensel, Sebastian Junges, Joost-Pieter Katoen, Tim Quatmann, and Matthias Volk. The probabilistic model checker Storm. *Int. J. Softw. Tools Technol. Transf.*, 24(4):589–610, 2022.
- [35] Enhyeok Jang, Youngmin Kim, Jeewoo Seo, Seungwoo Choi, and Won Woo Ro. Balancing thermal relaxation deviations of near-future quantum computing results via bit-inverted programs. *arXiv preprint arXiv:2502.20710*, 2025.
- [36] Sofiene Jerbi, Lea M Trenkwalder, Hendrik Poulsen Nautrup, Hans J Briegel, and Vedran Dunjko. Quantum enhancements for deep reinforcement learning in large spaces. *PRX Quantum*, 2(1):010328, 2021.

- [37] Peng Jin, Yang Wang, and Min Zhang. Efficient LTL model checking of deep reinforcement learning systems using policy extraction. In *SEKE*, pages 357–362. KSI Research Inc., 2022.
- [38] Jawaher Kaldari, Shehbaz Tariq, Saif Al-Kuwari, Samuel Yen-Chi Chen, Symeon Chatzinotas, and Hyundong Shin. Quantum reinforcement learning: Recent advances and future directions. *arXiv preprint arXiv:2510.14595*, 2025.
- [39] Yafim Kazak, Clark W. Barrett, Guy Katz, and Michael Schapira. Verifying deep-rl-driven systems. In *NetAI@SIGCOMM*, pages 83–89. ACM, 2019.
- [40] Gyu Seon Kim, Samuel Yen-Chi Chen, Soohyun Park, and Joongheon Kim. Quantum reinforcement learning for coordinated satellite systems. In *ICASSP*, pages 1–5. IEEE, 2025.
- [41] Georg Kruse, Rodrigo Coelho, Andreas Rosskopf, Robert Wille, and Jeanette Miriam Lorenz. Benchmarking quantum reinforcement learning. *arXiv preprint arXiv:2502.04909*, 2025.
- [42] Ryeonggu Kwon and Gihwon Kwon. Optimization of state clustering and safety verification in deep reinforcement learning using kmeans++ and probabilistic model checking. *IEEE Access*, 13:28085–28097, 2025.
- [43] Chuan-Feng Li, Yong-Sheng Zhang, Yun-Feng Huang, and Guang-Can Guo. Quantum strategies of quantum measurements. *Physics Letters A*, 280(5-6):257–260, 2001.
- [44] Yanling Lin, Ji Guan, Wang Fang, Mingsheng Ying, and Zhaofeng Su. Veriqr: A robustness verification tool for quantum machine learning models. In *FM (1)*, volume 14933 of *Lecture Notes in Computer Science*, pages 403–421. Springer, 2024.
- [45] Bo Lv. Supply chain resilience modeling based on dynamic hypergraph and quantum reinforcement learning for low-altitude-ground networks. *Transportation Research Part E: Logistics and Transportation Review*, 204:104458, 2025.
- [46] Evan R MacQuarrie, Christoph Simon, Stephanie Simmons, and Elicia Maine. The emerging commercial landscape of quantum computing. *Nature Reviews Physics*, 2(11):596–598, 2020.
- [47] Nicolas Maring, Andreas Fyrrillas, Mathias Pont, Edouard Ivanov, Eric Bertasi, Mario Valdivia, and Jean Senellart. One nine availability of a photonic quantum computer on the cloud toward hpc integration. In *2023 IEEE International Conference on Quantum Computing and Engineering (QCE)*, volume 2, pages 112–116. IEEE, 2023.
- [48] Eñaut Mendiluze Usandizaga, Shaukat Ali, Tao Yue, and Paolo Arcaini. Quantum circuit mutants: Empirical analysis and recommendations. *Empirical Software Engineering*, 30(3):100, 2025.
- [49] Nico Meyer, Julian Berberich, Christopher Mutschler, and Daniel D. Scherer. Robustness and generalization in quantum reinforcement learning via lipschitz regularization. *CoRR*, abs/2410.21117, 2024.
- [50] Nico Meyer, Christian Ufrecht, Maniraman Periyasamy, Daniel D Scherer, Axel Plinge, and Christopher Mutschler. A survey on quantum reinforcement learning. *arXiv preprint arXiv:2211.03464*, 2022.
- [51] Kosuke Mitarai, Makoto Negoro, Masahiro Kitagawa, and Keisuke Fujii. Quantum circuit learning. *Physical Review A*, 98(3):032309, 2018.
- [52] Enrique Moguel, Javier Rojo, David Valencia, Javier Berrocal, José García-Alonso, and Juan Manuel Murillo. Quantum service-oriented computing: current landscape and challenges. *Softw. Qual. J.*, 30(4):983–1002, 2022.
- [53] Asmar Muqet, Shaukat Ali, and Paolo Arcaini. Quiet: A tool for sampling-based quantum noise error mitigation. *IEEE Software*, 2025.
- [54] Asmar Muqet, Hassan Sartaj, Aitor Arrieta, Shaukat Ali, Paolo Arcaini, Maite Arratibel, Julie Marie Gjølby, Narasimha Raghavan Veeraragavan, and Jan F Nygård. Assessing quantum extreme learning machines for software testing in practice. *arXiv preprint arXiv:2410.15494*, 2024.
- [55] Juan Murillo, Jose Garcia-Alonso, Enrique Moguel, Johanna Barzen, Frank Leymann, and Shaukat Ali. Quantum software engineering: Roadmap and challenges ahead. *ACM Trans. Softw. Eng. Methodol.*, 2025.
- [56] Michael A Nielsen and Isaac L Chuang. *Quantum computation and quantum information*. Cambridge university press, 2010.
- [57] Dipesh Niraula, Jamalina Jamaluddin, Martha M Matuszak, Randall K Ten Haken, and Issam El Naqa. Quantum deep reinforcement learning for clinical decision support in oncology: application to adaptive radiotherapy. *Scientific reports*, 11(1):23545, 2021.
- [58] Noah H Oldfield, Christoph Laaber, Tao Yue, and Shaukat Ali. Faster and better quantum software testing through specification reduction and projective measurements. *ACM Transactions on Software Engineering and Methodology*, 34(7):1–39, 2025.

- [59] Koustubh Phalak and Swaroop Ghosh. Qualiti: Quantum machine learning hardware selection for inferencing with top-tier performance. In *2025 38th International Conference on VLSI Design and 2024 23rd International Conference on Embedded Systems (VLSID)*, pages 296–301. IEEE, 2025.
- [60] PRISM. PRISM Manual. www.prismmodelchecker.org, 2023. Accessed: 03/14/2024.
- [61] Minati Rath and Hema Date. Quantum data encoding: A comparative analysis of classical-to-quantum mapping techniques and their impact on machine learning accuracy. *EPJ Quantum Technology*, 11(1):72, 2024.
- [62] Denis Rosset, Cyril Branciard, Nicolas Gisin, and Yeong-Cherng Liang. Entangled states cannot be classically simulated in generalized bell experiments with quantum inputs. *New Journal of Physics*, 15(5):053025, 2013.
- [63] André Sequeira, Luis Paulo Santos, and Luis Soares Barbosa. Policy gradients using variational quantum circuits. *Quantum Machine Intelligence*, 5(1):18, 2023.
- [64] Akash Sinha, Antonio Macaluso, and Matthias Klusch. Nav-q: quantum deep reinforcement learning for collision-free navigation of self-driving cars. *Quantum Mach. Intell.*, 7(1):19, 2025.
- [65] Andrea Skolik, Sofiene Jerbi, and Vedran Dunjko. Quantum agents in the gym: a variational quantum algorithm for deep q-learning. *Quantum*, 6:720, 2022.
- [66] Andrea Skolik, Stefano Mangini, Thomas Bäck, Chiara Macchiavello, and Vedran Dunjko. Robustness of quantum reinforcement learning under hardware errors. *EPJ Quantum Technology*, 10(1):1–43, 2023.
- [67] Richard S Sutton and Andrew G Barto. *Reinforcement learning: An introduction*. MIT press, 2018.
- [68] Erik Terres Escudero, Danel Arias Alamo, Oier Mentxaka Gómez, and Pablo García Bringas. Assessing the impact of noise on quantum neural networks: An experimental analysis. In *HAIS*, volume 14001 of *Lecture Notes in Computer Science*, pages 314–325. Springer, 2023.
- [69] Peter Vamplew, Benjamin J. Smith, Johan Källström, Gabriel de Oliveira Ramos, Roxana Radulescu, Diederik M. Roijers, Conor F. Hayes, Fredrik Heintz, Patrick Mannion, Pieter J. K. Libin, Richard Dazeley, and Cameron Foale. Scalar reward is not enough: a response to silver, singh, precup and sutton (2021). *AAMAS*, 36(2):41, 2022.
- [70] Xinyi Wang, Shaukat Ali, and Paolo Arcaini. Bqtmizer: A tool for test case minimization with quantum annealing. *IEEE Software*, 2025.
- [71] Xinyi Wang, Shaukat Ali, and Davide Taibi. The landscape of quantum software testing tools publisher. *IEEE Software*, 42, 2025.
- [72] Xinyi Wang, Qinghua Xu, Paolo Arcaini, Shaukat Ali, and Thomas Peyrucain. Quantum machine learning-based test oracle for autonomous mobile robots. *arXiv preprint arXiv:2508.02407*, 2025.
- [73] Yu Wang, Nima Roohi, Matthew West, Mahesh Viswanathan, and Geir E. Dullerud. Statistically model checking PCTL specifications on markov decision processes via reinforcement learning. In *CDC*, pages 1392–1397. IEEE, 2020.
- [74] Ronald J Williams. Simple statistical gradient-following algorithms for connectionist reinforcement learning. *Machine learning*, 8(3):229–256, 1992.
- [75] Sau Lan Wu, Jay Chan, Wen Guan, Shaojun Sun, Alex Wang, Chen Zhou, Miron Livny, Federico Carminati, Alberto Di Meglio, Andy CY Li, et al. Application of quantum machine learning using the quantum variational classifier method to high energy physics analysis at the lhc on ibm quantum computer simulator and hardware with 10 qubits. *Journal of Physics G: Nuclear and Particle Physics*, 48(12):125003, 2021.
- [76] He Zhu, Zikang Xiong, Stephen Magill, and Suresh Jagannathan. An inductive synthesis framework for verifiable reinforcement learning. In *PLDI*, pages 686–701. ACM, 2019.